JOURNAL OF Applied Polymer SCIENCE

Sulfonated Polyimide/Chitosan Composite Membrane for Vanadium Redox Flow Battery: Membrane Preparation, Characterization, and Single Cell Performance

Mingzhu Yue,[1,2] Yaping Zhang,[1,2] Lei Wang[1,2]

[1]Engineering Research Center of Biomass Materials, Ministry of Education, Mianyang 621010, People's Republic of China
[2]Department of Chemistry, School of Materials Science and Engineering, Southwest University of Science and Technology, Mianyang 621010, People's Republic of China
Correspondence to: Y. Zhang (E-mail: zhangyaping@swust.edu.cn)

ABSTRACT: A novel sulfonated polyimide/chitosan (SPI/CS) composite membrane was prepared from self-made SPI (50% of sulfonation degree) through an immersion and self-assembly method, which was successfully applied in vanadium redox flow battery (VRB). The proton conductivity of SPI/CS composite membrane is effectively improved compared to the plain SPI membrane. The VO^{2+} permeability coefficient across SPI/CS composite membrane is 1.12×10^{-7} cm^2 min^{-1}, which is only one tenth of that of Nafion® 117 membrane. Meanwhile, the proton selectivity of SPI/CS composite membrane is about eight times higher than that of Nafion® 117 membrane. In addition, the oxidative stability SPI/CS composite membrane is superior to that of pristine SPI membrane. The VRB single cell using SPI/CS composite membrane showed higher energy efficiency (88.6%) than that using Nafion® 117 membrane, indicating that SPI/CS composite membrane is a promising proton conductive membrane for VRB application. © 2012 Wiley Periodicals, Inc. J. Appl. Polym. Sci. 000: 000–000, 2012

KEYWORDS: polyimides; membranes; composites; vanadium redox flow battery

Received 12 January 2012; accepted 1 May 2012; published online
DOI: 10.1002/app.38007

INTRODUCTION

The vanadium redox flow battery (VRB) has attracted considerable attention for its long cycle life, flexible design, fast response time, deep discharge capability, low cost, and low pollution.[1–4] In VRB, VO_2^+/VO^{2+} is employed as a positive electrolyte; whereas V^{3+}/V^{2+} is as a negative one. The following reactions (1–2) can be used to interpret the charge and discharge phenomena occurred in

$$\text{Positive half-cell:} \quad VO^{2+} + H_2O \underset{\text{discharge}}{\overset{\text{charge}}{\rightleftharpoons}} VO_2^+ + 2H^+ + e^- \quad (1)$$

$$\text{Negative half-cell:} \quad V^{3+} + e^- \underset{\text{discharge}}{\overset{\text{charge}}{\rightleftharpoons}} V^{2+} \quad (2)$$

Proton conductive membrane is one of the key components for VRB, which effectively prevents the crossover of catholyte and anolyte and provides a conductive pathway to complete the circuit during the passage of current. An ideal proton conductive membrane for VRB should possess high proton conductivity, low vanadium ion permeability, excellent chemical stability, high mechanical strength, and low price.[5] Nevertheless, most early commercial membranes are unsuitable for VRB application due to their poor stabilities in pentavalent vanadium ion (VO_2^+) solution.[6] Up to now, the perfluorinated sulfonic acid membranes such as Nafion® membranes (Dupont, USA) have been widely used in VRB system owing to their high proton conductivities and excellent chemical stabilities. However, Nafion® membranes also reveal such disadvantages as high vanadium ion permeabilities and high cost, which limit their large-scale commercial application in VRB system.[7] Therefore, developing novel proton conductive membranes with high proton conductivity, good chemical stability, low vanadium ion permeability, and low cost is significantly important and highly needed for large-scale industrialization of VRB.

Hopefully, some suitable proton conductive membranes with excellent cell performance and low cost have been developed for VRB application.[8–13] For instance, some aromatic polymers[14–19] were functionalized to improve proton conductivity by introducing sulfonic acid group. Compared with Nafion® membranes, the vanadium ion permeabilities of these membranes have been sharply decreased and they are of quite lower cost. However, these newly developed proton conductive membranes also exhibit some disadvantages including low mechanical

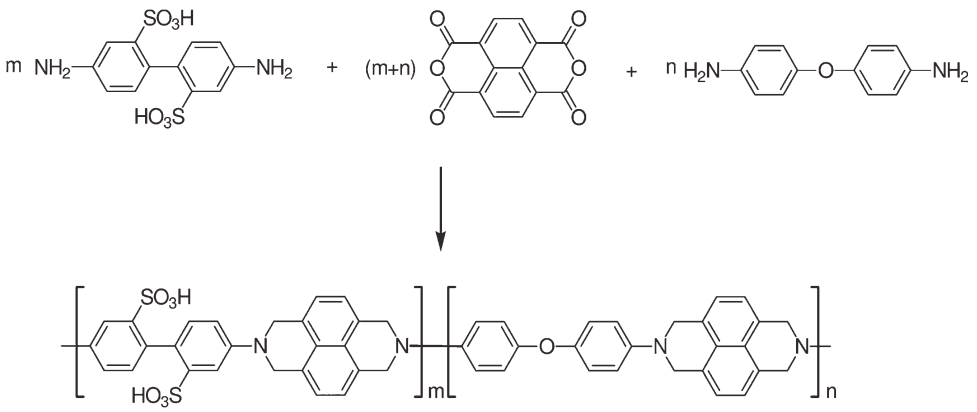

Scheme 1. Synthesis of sulfonated polyimide.

strength and oxidative stability. Consequently, other aromatic polymer membranes should be sought for VRB application.

Recently, a novel proton conductive membrane prepared from sulfonated polyimide (SPI) for VRB application was developed in our laboratory.[20] The obtained SPI membrane had lower vanadium ion permeability and reasonable proton conductivity, demonstrating its promising application in VRB. However, the plain SPI membrane also showed low oxidative stability like other membranes made of a single aromatic polymer. Therefore, to continue our previous work and prepare a novel environmental friendly proton conductive membrane, a novel acid–base polymer composite membrane based on SPI and chitosan (CS) was prepared by an immersion and self-assembly method. The physico–chemical properties of SPI/CS composite membrane and the performance of a single cell for VRB application were also investigated. Compared with our previous study,[20] the novelties of this new route are: (1) CS was introduced into the membrane as an environmental friendly acid–base polymer precursor; (2) the sulfuric acid was used as a crosslinker to increase the mechanical strength and decrease the vanadium ion permeability of the SPI/CS composite membrane.

EXPERIMENTAL

Materials

The 1,4,5,8-naphthalenetetracarboxylic dianhydride (NTDA) was supplied by Beijing Multi. Tech. The 4,4′-diamino-biphenyl 2,2′-disulphonic acid (BDSA) was bought from Quzhou Rainful Chem. The 4,4′-oxydianiline (ODA) was bought from Beshine Chem. Tech. Vanadyl sulfate ($VOSO_4$) was purchased from Shanghai Lvyuan Fine Chem. Plant. M-cresol was obtained from Shanghai Kefeng Chem. Reagent. Triethylammonium (TEA) and other reagents were obtained from Chengdu Kelong Chemical Reagent.

Preparation of SPI Membrane

The random SPI was prepared by a conventional method.[21] The sulfonation degree of SPI was controlled to be 50% to obtain reasonable proton conductivity and mechanical strength according to our earlier research.[20] The preparation procedure can be described as follows: 0.28 g of 4,4′-diamino-biphenyl 2,2′-disulphonic acid (BDSA) (≈1.0 mmol), 0.20 g of triethylammonium (TEA), and 10 mL of m-cresol were added into a three-necked round bottom flask under nitrogen atmosphere. The mixture was stirred vigorously at room temperature until BDSA was dissolved completely. Then 0.54 g of 1,4,5,8-naphthalenetetracarboxylic dianhydride (NTDA) (≈2.0 mmol), 0.20 g of 4,4′-oxydianiline (ODA) (≈1.0 mmol), and 0.49 g of benzoic acid were added drop wise. The mixture was stirred vigorously for several minutes, followed by heating it at 80°C for 4 h and at 180° for 20 h, respectively. After cooling down to 80°C, 5 mL m-cresol was added to dilute the viscous solution. Then the mixed solution was poured into 100 mL acetone to separate the reaction product. The fiber-like precipitate product was filtered and washed with acetone for several times, and then dried at 80°C for 24 h. Finally, the SPI (in TEA salt form) was obtained.

The above-prepared SPI (in TEA salt form) was added into a m-cresol solution (8 wt %), then the mixed solution was casted onto a clean glass. After dried at 60°C for 20 h and 80°C for 2 h, a SPI membrane (in TEA salt form) was obtained. Subsequently, the membrane was soaked in a 1.0*M* aqueous H_2SO_4 solution at room temperature for 24 h and thoroughly washed with deionized water to remove sulfuric acid on the membrane surface. Thus, a SPI membrane in proton form was obtained, and its thickness was about 45 μm. The corresponding reaction can be described in Scheme 1.

Preparation of SPI/CS Composite Membrane

Chitosan solution (2 (w/v) %) was prepared by dissolving certain chitosan powder in 2 (w/v) % acetic acid solution at 70°C. After the chitosan powder was dissolved completely, bubbles in chitosan solution were removed, and then the chitosan solution was kept quiescent at room temperature.

The SPI/CS composite membrane was prepared by an immersion and self-assembly method as following: the SPI membrane (in proton form) was immersed in above-prepared 2 (w/v) % chitosan solution for 24 h and then dried at 50°C for 6 h. Followed, the membrane was crosslinked with 2.0*M* sulfuric acid for 10 h. After dried at 50°C for 12 h, the SPI/CS membrane was obtained. Scheme 2 shows the crosslinking between CS and sulfuric acid,[22] and Scheme 3 shows the interaction between SPI and crosslinked CS.

Characterization of Membranes

Fourier transform infrared spectroscopy (FT-IR) spectra (4000–650 cm^{-1}, resolution 4 cm^{-1}) were recorded using Nicolet-5700 spectrometer.

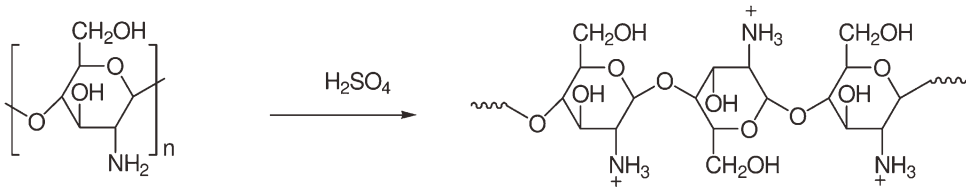

Scheme 2. Crosslinking reaction of chitosan with sulfuric acid.[22]

The surface and cross-sectional images were observed using a FEI scanning electron microscope (SEM), and the cross-section of membranes was obtained by the freeze-fracture technique in liquid nitrogen.

The thermal stability was determined by a thermogravimetric analyzer (SDT Q600) in 100 mLmin^{-1} nitrogen atmosphere with a heating rate of 10°C min^{-1}.

The weight percent of CS with respect to SPI in the SPI/CS composite membrane was calculated by the following eq. (3).

$$\text{CS content}(\%) = \frac{m' - m}{m} \times 100 \tag{3}$$

where m and m' are the weights of the pristine SPI membrane and the SPI/CS composite membrane (g), respectively.

The water uptake (WU) was defined as the ratio of the weight of absorbed water to that of a dry membrane. The WU was determined in the following way: a membrane was immersed in deionized water for 24 h until completely swollen, then the membrane was taken out and wiped off the surface moisture with a tissue paper and quickly weighed. The wet membrane was dried at 60°C until a constant weight was reached. The WU was calculated according to eq. (4):

$$\text{WU}(\%) = \frac{W_{\text{wet}} - W_{\text{dry}}}{W_{dry}} \times 100 \tag{4}$$

where W_{wet} and W_{dry} are the weights of wet and dry membrane (g), respectively.

The swelling ratio was determined by the dimensional change as linear expansion ratio (ΔL). It was calculated by the following eq. (5):

$$\Delta L(\%) = \frac{L_{\text{wet}} - L_{\text{dry}}}{L_{dry}} \times 100 \tag{5}$$

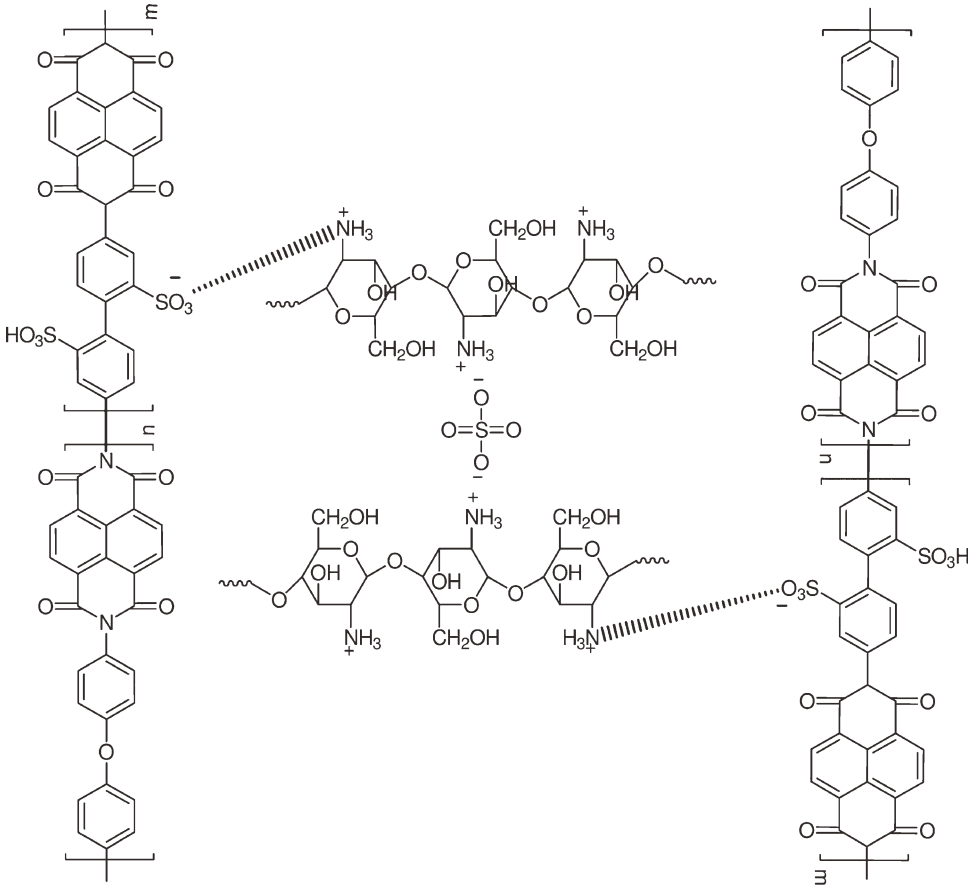

Scheme 3. Interaction between crosslinked chitosan and sulfonated polyimide.

Applied Polymer SCIENCE

where L_{wet} and L_{dry} are the length of wet and dry membrane (cm), respectively.

The ion exchange capacity (IEC) was measured by a conventional titration method. A dry membrane was weighed and immersed into a 1.0*M* NaCl solution for 24 h to exchange proton with sodium ion. The membrane was then taken out and washed with deionized water, and the remained solution was titrated using 0.05*M* NaOH solution with phenolphthalein as an indicator. The IEC was determined by eq. (6):

$$\mathrm{IEC} = \frac{C_{\mathrm{NaOH}} \cdot V_{\mathrm{NaOH}}}{W_{\mathrm{dry}}} \tag{6}$$

where C_{NaOH} and V_{NaOH} are the concentration (mol L^{-1}) and volume (mL) of consumed NaOH solution, respectively.

The oxidative stability was measured by a similar method with that presented in the literature,[19] namely, the weight change of the membrane before and after immersed in 0.5*M* VO_2^+ and 2.0*M* H_2SO_4 mixed aqueous solution was determined. The weight loss of the membrane was calculated by eq. (7).

$$\text{weight loss}(\%) = \frac{m_0 - m_1}{m_0} \times 100 \tag{7}$$

where m_0 and m_1 are the weights of the dry membrane (g) before and after immersed in the oxidation solution for 20 days, respectively.

The proton conductivity was determined using four-point-probe electrochemical impedance spectroscopy. A membrane was rinsed in deionized water for 24 h before measurement, then fixed in a measuring cell which is made from teflon material consisted of two stainless steel flat outer current-carrying electrodes and two platinum wire inner potential-sensing electrodes.[23] The membrane in 1-cm wide and 4-cm long was mounted on the cell. The impedance was measured using Princeton 2273 electrochemical workstation at galvanostatic mode with ac current amplitude of 5 mA over frequency range from 1.0 Hz to 100 kHz. The proton conductivity was calculated using eq. (8):

$$\sigma = \frac{L}{R \cdot S \cdot d} \tag{8}$$

where σ is the proton conductivity (S cm^{-1}), R is the obtained membrane resistance (Ω), L is the distance between the two platinum wires (cm), S and d are the width (cm) and thickness ($\times 10^{-4}$ cm) of the membrane, respectively.

The permeability of vanadium ions across the membrane was measured with the equipment depicted in Figure 1, which has two identical compartments with a membrane as separator. The left compartment was filled with 120 mL of 1.0*M* $VOSO_4$ in 2.0*M* H_2SO_4 solution, and the right one was 120 mL of 1.0*M* $MgSO_4$ in 2.0*M* H_2SO_4 solution. $MgSO_4$ here was used to balance the ionic strength of two solutions and reduce the osmotic pressure effect.[24] The effective membrane area was 5.31 cm^2. The sample solution was taken out from the right compartment at a regular time and the concentration of VO^{2+} was

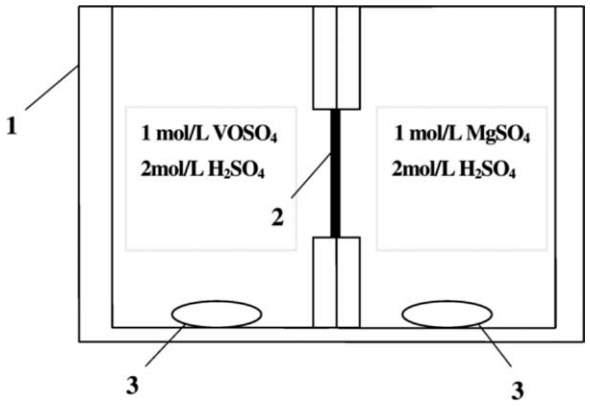

Figure 1. Schematic configuration of the device for measurement of VO^{2+} permeability across the membrane. (1) Teflon tank, (2) Membrane, (3) Magnetic stirrer.

determined by Ultraviolet–visible spectroscopy (UV-1200). The change of VO^{2+} concentration in the left compartment was quite small during the whole experiment and can be negligible. Consequently, VO^{2+} concentration in the right compartment as a function of time was given by the following eq. (9):

$$\frac{dC_{R(t)}}{dt} = \frac{A \cdot P}{V_R \cdot d}(C_L - C_{R(t)}) \tag{9}$$

where C_L is VO^{2+} concentration in the left compartment (mol L^{-1}), $C_{R(t)}$ is VO^{2+} concentration (mol L^{-1}) in the right compartment at diffusion time t (min). V_R is the volume of the right compartment (cm^3). A (cm^2) and d ($\times 10^{-4}$ cm) are the area and the thickness of the membrane, respectively. P is VO^{2+} permeability coefficient of the membrane (cm^2 min^{-1}). And an assumption that the P is independent of vanadium ion concentration is made here.

Single Cell Testing

The charge-discharge test of VRB was conducted using a similar method reported in literatures,[19,25] in which the membrane was sandwiched between the positive and negative half cell. The electrolytes used were 30 mL of 1.5 M V^{2+}/V^{3+} in 3.0*M* H_2SO_4 solution as cathodic electrolyte, and 30 mL of 1.5*M* VO^{2+}/VO_2^+ in 3.0*M* H_2SO_4 solution as anodic electrolyte, respectively. They were pumped through the cell during the test at room temperature. The VRB single cell test was carried out at a charge-discharge current density of 40 mA cm^{-2}. To avoid the corrosion of the graphite felt electrode and graphite polar plates, the upper limit voltage for charge and the lower limit voltage for discharge were 1.8 and 0.8 V, respectively. The charge–discharge test of VRB single cell was carried out by CT-3008-5V/3A battery testing system. The coulombic efficiency (CE), the voltage efficiency (VE), and the energy efficiency (EE) of the single cell were calculated by following eqs. (10)–(12):

$$\mathrm{CE} = \frac{C_{\mathrm{dis}}}{C_{\mathrm{ch}}} \times 100\% \tag{10}$$

$$\mathrm{VE} = \frac{\bar{V}_{\mathrm{dis}}}{\bar{V}_{\mathrm{ch}}} \times 100\% \tag{11}$$

$$EE = CE \times VE \quad (12)$$

where C_{dis} and C_{ch} are the discharge and the charge capacity, respectively; $\overline{V_{dis}}$ and $\overline{V_{ch}}$ are the average discharge and the charge voltage, respectively.

RESULTS AND DISCUSSION

Structure, Morphological, and Thermal Analysis

The chemical structure can be availably confirmed by FT-IR spectra. Figure 2 illustrates the infrared reflectance spectra of the membranes SPI/CS crosslinked with sulfuric acid (SPI/CS in this work), SPI/CS without crosslinking with sulfuric acid, pristine CS, and CS crosslinked with sulfuric acid, respectively. The characteristic peaks located at 1650.6 and 1589.4 cm^{-1} represent Amide I and II of pristine CS, individually. However, Amide I and II peaks of SPI/CS membrane without crosslinked with sulfuric acid shift to lower wavenumbers, i.e., 1633.1 and 1530.3 cm^{-1} separately, owing to the ionic interaction between the sulfonic acid groups of SPI and the amino groups of CS. Likely, such an ionic interaction between the sulfonic acid groups of sulfuric acid and the amino groups of CS also exists. Consequently, the change of Amide I and II peaks of SPI/CS membrane is the result of above two aspects. And these results also confirm the formation of products shown in Schemes 2 and 3. In fact, our experimental results are in agreement with that reported by Smitha et al.,[26] and such characteristic peak shifts of Amides I and II were also observed for SPSF/CS composite membranes.

Meanwhile, the infrared transmission spectra of SPI/CS and SPI membranes were also determined to get more information about the structure of membranes, and relative results were depicted in Figure 3. The pristine SPI membrane shows the stretching bands at 1713.0, 1672.7, 1348.2, 1099.5, and 1031.4 cm^{-1}, which are attributed to asymmetric and symmetric carbonyl groups, imide of the six-membered naphthalene imide rings, and asymmetric and symmetric sulfonic acid groups, respectively. These results justify our success synthesis of SPI. In the meantime, these absorbance peaks can also be observed for SPI/CS composite membrane, verifying the presence of SPI on the SPI/CS composite membrane. In addition, the IR spectrum of SPI/CS composite membrane also shows a shift in the band representing Amide I of CS to a lower wavenumber at 1631.4 cm^{-1}, which further confirms the formation of ionic bond between SPI and CS. Furthermore, two characteristic peaks at 2925.1 and 2854.2 cm^{-1} attributed to —CH_2— of CS are observed on SPI/CS composite membrane, confirming the presence of CS on the composite membrane. In short, the SPI/CS composite membrane is successfully prepared according to Figures 2–3.

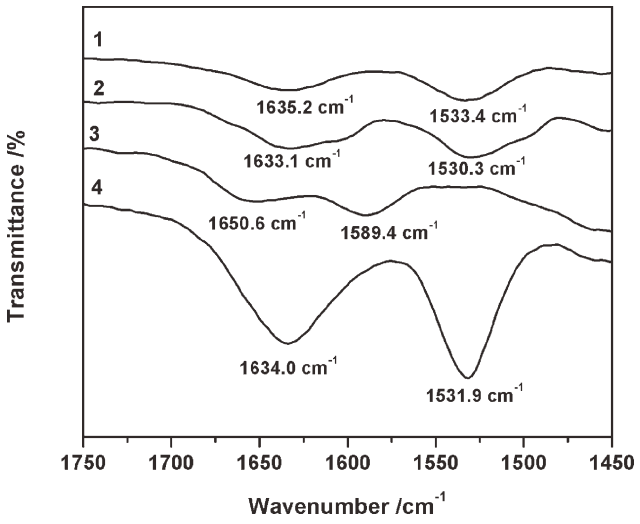

Figure 2. The infrared reflectance spectra of the membranes: (1) SPI/CS crosslinked with sulfuric acid (SPI/CS in this work), (2) SPI/CS without crosslinking with sulfuric acid, (3) Pristine CS, (4) CS crosslinked with sulfuric acid.

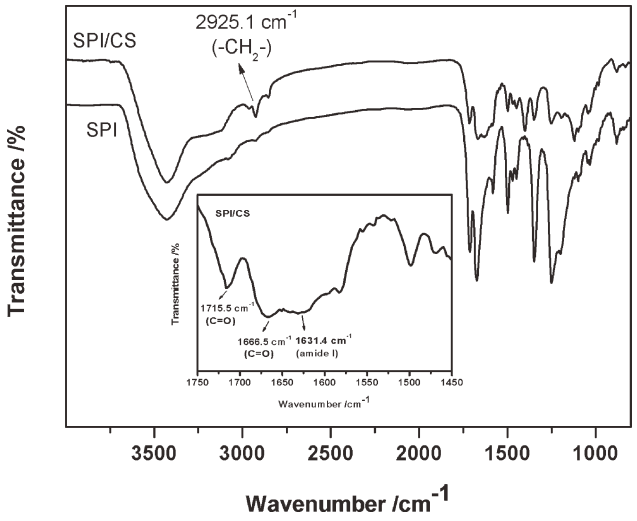

Figure 3. The infrared transmission spectra of SPI, SPI/CS membranes.

As is known, possessing a perfect surface image is very important for the proton conductive membrane for VRB application. Figure 4(a,b) show the images of SPI and SPI/CS composite membranes, from which the homogeneous smooth surfaces can be always seen. To present more micro image information, the SEM images of the surface and cross-section of SPI and SPI/CS membranes were also illustrated in Figure 5(a–d). As shown in Figure 5(a,b), there are no pores or defects in both membrane surfaces. However, the surface of SPI/CS membrane appears a little rougher when compared with that of pure SPI membrane due to the introduction of CS. Especially, the SPI/CS composite membrane still exhibits uniform, dense morphology and there is no obvious phase separation at 5000× magnification. As for cross-section SEM images shown in Figure 5(c,d), three layers including SPI central layer and two thin CS layers at both sides of SPI can be apparently observed for SPI/CS composite membrane. Furthermore, these three layers are closely combined, and no crack at the interface of any two layers can be found. These outcomes demonstrate that the CS is just adsorbed onto the surface and the SPI/CS composite membrane has been successfully prepared via the immersion and self-assembly method.

The thermal stability of CS, SPI, and SPI/CS membranes was measured by thermogravimetry analysis (TGA) and the related

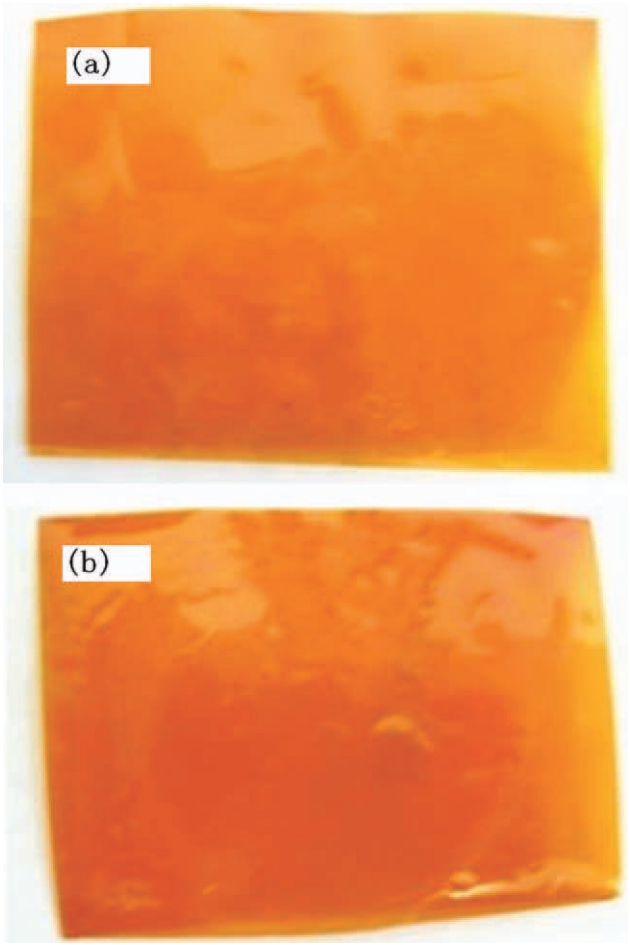

Figure 4. The surface images of membranes: (a) SPI, (b) SPI/CS. [Color figure can be viewed in the online issue, which is available at wileyonlinelibrary.com.]

curves are shown in Figure 6. The CS membrane presents two major degradation stages within 30–100°C and 280–320°C. The first degradation stage is the evaporation of absorbed water at the membrane surface. The second one can be ascribed to the degradation of CS main chain.[27] Differently, the TGA curve of SPI membrane exhibits three-step weight loss pattern. The first weight loss is observed around 30–100°C, which is attributed to the loss of absorbed moisture by the highly hydrophilic sulfonic acid groups. The second one is observed within 300–450°C, which is the decomposition of sulfonic acid group. The third beyond 550°C indicates the further decomposition of SPI main chain. For SPI/CS composite membrane, its TGA curve follows a similar change trend as that of SPI membrane, suggesting that the combination of SPI with CS doesn't decrease the thermal stability of SPI/CS composite membrane too much. Meanwhile, such a combination of SPI with CS overcomes the lower thermal stability of pure CS membrane. This observation reveals that the composite of two different membranes enhances their individual thermal stabilities.

Physicochemical Properties

Fundamental physicochemical properties of SPI, SPI/CS, and Nafion® 117 membranes were measured to evaluate the membrane performance, and relative results are summarized in Table I. The weight percent of CS with respect to SPI in the SPI/CS composite membrane is 5.64 wt %.

The ratio of the molar content of ion exchange group to the weight of dry membrane is identified as ion exchange capacity (IEC), which is depended on the content of sulfonic acid group having free proton in polymer membrane. IEC plays an important role in proton conductive membrane, which directly or indirectly influences proton conductivity and water uptake of membrane. The IEC value follows such an order: SPI/CS (1.65 mequiv g^{-1}) > SPI (1.61 mequiv g^{-1}) > Nafion® 117 (1.14 mequiv g^{-1}). Among them SPI/CS composite membrane reveals the highest IEC value. This trend can be ascribed to the incorporation of sulfuric acid for crosslinking during the preparation of the composite membrane. Moreover, the IEC value of SPI/CS composite membrane increases slightly by comparison with that of pristine SPI membrane, suggesting that the combination of SPI with CS doesn't increase its IEC value greatly. This is attributed to be the neutralization of free sulfonic acid group of SPI by the amino group in the base polymer CS. Accordingly, the acid–base interaction between SPI and CS by ionic bond is formed.

Water uptake (WU) is another important performance parameter for proton conductive membrane, which is closely related with the dimensional stability and proton conductivity of investigated membranes. The WUs of various kinds of membranes were evaluated and the results were also presented in Table I. The pure SPI membrane shows a water uptake of 41.40%, meanwhile the water uptake of SPI/CS composite membrane is 28.66%. The decreased water uptake of SPI/CS composite membrane compared to that of SPI membrane can be put down to two reasons.[28] The one is related to the effect of crosslinking between CS and sulfuric acid. As the membrane is crosslinked, it becomes more rigid and structurally compact, then free volume available for water molecules decreases accordingly. The other can be ascribed to the effect of ionic interaction between crosslinked CS and SPI. As a result, the number of free sulfonic acid group is decreased, leading to the decrease of absorbed water in this type of membrane. Based on these results, it can be deduced that the high IEC and low WU will result in low vanadium permeability for SPI/CS membrane, which can be further verified by the following VO^{2+} permeability data.

The swelling ratio is also considered as one crucial parameter affecting proton transport and dimensional stability for proton conductive membrane application. Currently, it is well accepted that proper water uptake conduces to the proton transportation across membranes. In contrast, excessive high water uptake will lead to serious dimensional change of membranes and even marked mechanical breakage of membranes in VRB system. Therefore, it is necessary to control the water uptake of proton conductive membranes. Table I also lists the dimensional change of SPI, SPI/CS, and Nafion® 117 membranes. The dimensional change follows such an order: SPI (4.80%) < SPI/CS (6.66%) < Nafion® 117(10.90%). Obviously, SPI/CS composite membrane is slightly swollen compared with that of pristine SPI membrane. When the CS is added onto the SPI membrane through the immersion and self-assembly method, the ionic interaction is formed between SPI and CS, causing the SPI/CS composite

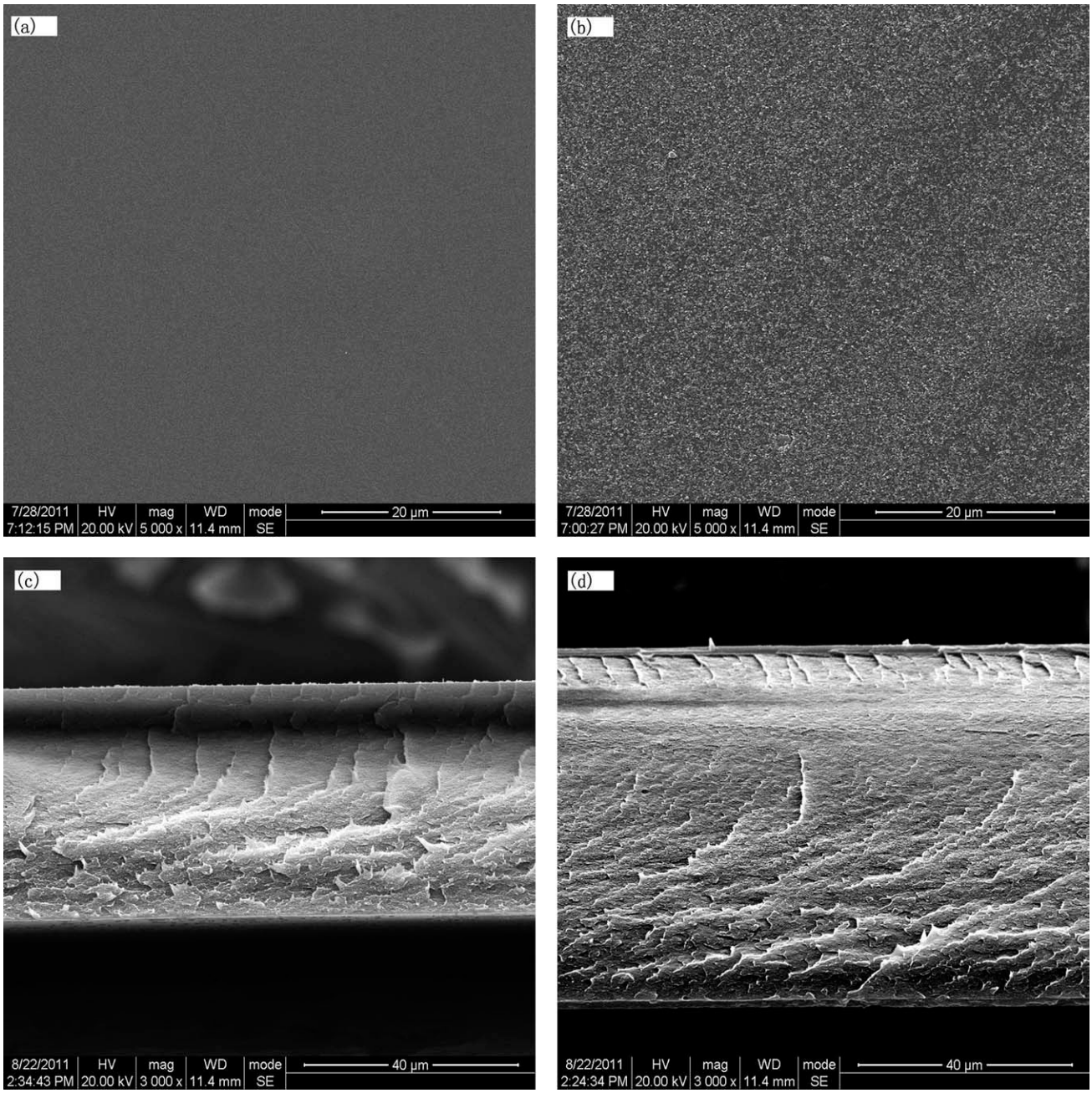

Figure 5. SEM images of surfaces of membranes: (a) SPI, (b) SPI/CS; SEM images of cross-sections of membranes: (c) SPI, (d) SPI/CS.

membrane more compact and less swollen from the point of theoretical view. However, the experimental results show the opposite trend, that is, the SPI/CS membrane is more swollen than SPI membrane. The reason is that CS is highly hydrophilic and easily swollen, and such an effect is larger than above ionic interaction on the SPI/CS membrane. Nevertheless, the swelling of SPI/CS membrane is still markedly less than Nafion® 117 membrane, suggesting that the dimensional stability of SPI/CS membrane is better than that of Nafion® 117.

In addition, the oxidative stabilities of SPI, SPI/CS and Nafion® 117 membranes were investigated by weight loss in VO_2^+ solution at room temperature and the results were listed in Table I. To our surprise, SPI/CS composite membrane remains intact in VO_2^+ solution. Although the weight loss of SPI/CS membranes in VO_2^+ solution is a little higher than Nafion® 117 membrane, it is less than that of the pristine SPI membrane, indicating that the oxidative stability of SPI/CS membrane is largely promoted. Therefore, SPI/CS membrane can be used in the VO_2^+ solution of VRB system.

Proton Conductivity and VO^{2+} Permeability

It is necessary for proton conductivity membranes to have high proton conductivities as far as possible. Proton conductivity of membranes at room temperature was measured by

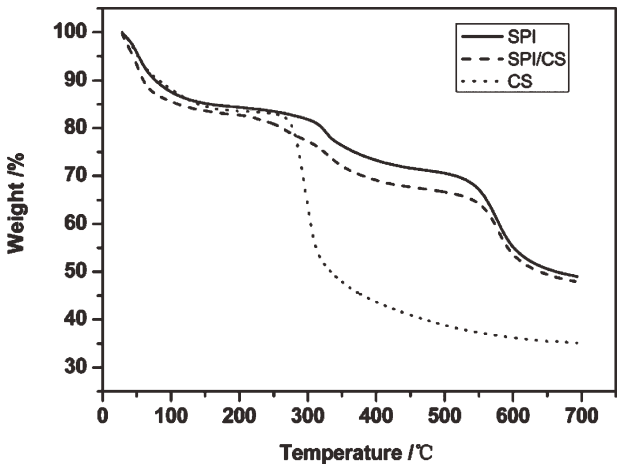

Figure 6. TGA curves of CS, SPI and SPI/CS membranes.

Electrochemical Impedance Spectroscopy (EIS) after immersing it in deionized water for 24 h.

Table II shows the proton conductivity of SPI, SPI/CS, and Nafion® 117 membranes, where the proton conductivity SPI/CS membrane is higher than that of plain SPI membrane. It is worth mentioning that the concentration of sulfuric acid used to crosslink the CS is 2.0*M*, which is not high enough to change the sulfonation degree of the SPI polymer. Thus, sulfuric acid was used only as crosslinking agent, and it is not clear its contribution to the proton conductivity. Therefore, the increase of conductivity value of the composite SPI/CS is mainly caused by the crosslinked reaction between CS and sulfuric acid. As mentioned above, high proton conductivity is largely depended on suitably high IEC. In fact, the SPI/CS composite membrane has higher proton conductivity, which is mainly due to its higher IEC through crosslinking with sulfuric acid[26] in comparison with plain SPI membrane in this work. Therefore, the proton conductivity of SPI/CS and SPI membranes are 3.94×10^{-2} S cm^{-1} and 3.02×10^{-2} S cm^{-1}, respectively.

However, although the IEC of SPI/CS (1.65 mequiv g^{-1}) is larger than that of Nafion® 117 membrane (1.14 mequiv g^{-1}), the conductivity of the SPI/CS (3.94×10^{-2} S cm^{-1}) is contrarily lower than that of Nafion® 117 membrane (6.41×10^{-2} S cm^{-1}). As a matter of fact, IEC is only one of the factors influencing the proton conductivity. Because Nafion® 117 membrane has unique hydrophilic–hydrophobic phase separation structure, which is quite favorite for its proton conductivity. Therefore, although the IEC is not so high, the proton conductivity is still very high for Nafion® 117 membrane. However, it should be pointed out that although the proton conductivity of SPI/CS membrane is lower than that of Nafion® 117 membrane, it is still in the same order ($\times 10^{-2}$ S cm^{-1}) with respect to that of Nafion® 117. Therefore, the SPI/CS composite membrane is a promising candidate for VRB application.

In addition, the vanadium ion permeability is one of the most important performance parameters of the proton conductive membrane for VRB, which represents the ability to effectively prevent the crossover of positive and negative electrolytes. To give an insight into the permeability of vanadium ion, the vanadium ion permeabilities of SPI, SPI/CS, and Nafion® 117 membranes were also measured. The dependency of VO^{2+} concentration in the right compartment as a function of time is shown in Figure 7. Based on the experimental data in Figure 7, the vanadium ion permeabilities for different membranes can be easily calculated from Eq. (9). From Table II it can be seen that the vanadium ion permeabilities of SPI and SPI/CS membranes are 1.89×10^{-7} cm^2 min^{-1} and 1.12×10^{-7} cm^2 min^{-1}, respectively. In contrast, the permeability of vanadium ion of Nafion® 117 membrane is 15.41×10^{-7} cm^2 min^{-1}. Apparently, SPI/CS composite membrane displays much higher vanadium ion barrier property than that of Nafion® 117. This finding demonstrated that SPI/CS composite membrane can effectively prevent the crossing of vanadium ion. Two dominating factors will be responsible for such a result. On one hand, the addition of CS layer onto the surface of SPI membrane blocks micropores in the SPI membrane and forms ionic interaction with SPI. On the other hand, the crosslinking of CS and sulfuric acid makes the membrane more rigid and structurally compact. As a result, the dense structure of SPI/CS composite membrane can effectively prevents the transportation of vanadium ions across the

Table I. Physicochemical Properties of SPI, SPI/CS, and Nafion® 117 Membranes

Membrane	CS content (%)	Thickness (μm)	WU (%)	Swelling ratio (%)	IEC (mequiv g^{-1})	Weight loss (%)
SPI	-	45	41.40	4.80	1.61	7.80
SPI/CS	**5.64**	50	28.66	6.66	1.65	5.56
Nafion® 117	-	175	18.60	10.90	1.14	2.31

Table II. Proton Conductivity, VO^{2+} Permeability Coefficient, and Proton Selectivity of SPI, SPI/CS, and Nafion® 117 Membranes

Membrane	Proton conductivity ($\times 10^{-2}$ S cm^{-1})	VO^{2+} Permeability coefficient ($\times 10^{-7}$ cm^2 min^{-1})	Proton selectivity [$\times(10^{-2}$ S $cm^{-1})/(10^{-7} cm^2$ $min^{-1})$]
SPI	3.02	1.89	1.60
SPI/CS	3.94	1.12	3.52
Nafion® 117	6.41	15.41	0.42

membrane. Consequently, the vanadium ion resistance of SPI/CS membrane is superior and the vanadium ion permeability of SPI/CS composite membrane reaches one order of magnitude lower than Nafion® 117 membrane, which is favorable for its application in VRB system.

The proton conductive membrane used in VRB should possess high proton conductivity and low vanadium ion permeability simultaneously. However, these two property parameters are opposite as usual. Consequently, a new parameter, proton selectivity, which is defined as the ratio of proton conductivity to vanadium ion permeability, is more reasonable to evaluate the comprehensive performance. The proton selectivities of various membranes were measured and listed in Table II. The proton selectivities of SPI, SPI/CS, and Nafion® 117 membranes follow such an order as: SPI/CS [3.52 × (10^{-2} S cm^{-1})/(10^{-7} cm^2 min^{-1})] > SPI [1.60 × (10^{-2} S cm^{-1})/($10^{-7}$$cm^2$ min^{-1})] > Nafion® 117 [0.42 × (10^{-2} S cm^{-1})/($10^{-7}$$cm^2$ min^{-1})]. Obviously, the proton selectivity of SPI/CS membrane is higher than that of Nafion® 117 membrane. In particular, the proton selectivity of SPI/CS composite membrane is as about eight times high as that of Nafion® 117 membrane, indicating that it is promising for VRB application.

The Performance of VRB Single Cell

The performance of VRB single cell with SPI, SPI/CS, and Nafion® 117 membranes at a charge–discharge current density of 40 mA cm^{-2} was investigated; the results are summarized in Table III. The single cell using SPI/CS membrane shows the voltage efficiency of 90.6%, which is only a little lower than that using Nafion® 117. This is caused by the lower proton conductivity of SPI/CS membrane than that of Nafion® 117. With regard to the coulombic efficiency, the single cell using SPI/CS membrane has higher value than that using Nafion® 117 membrane, indicating that the self-discharge of SPI/CS membrane is decreased largely. This result is also in agreement with the vanadium ion permeability data (shown in Figure 7 and Table II). In fact, as an indicator of energy loss in the charge–discharge process, energy efficiency is the key parameter to evaluate an energy storage system. As shown in Table III, the energy efficiency for SPI/CS membrane (88.6%) and that for Nafion® 117 membrane (86.9%) indicates the superior VRB performance by using SPI/CS instead of Nafion® 117. Based on these results, it can be further reasoned out that SPI/CS membrane is a promising substitute for Nafion® 117 used in VRB system.

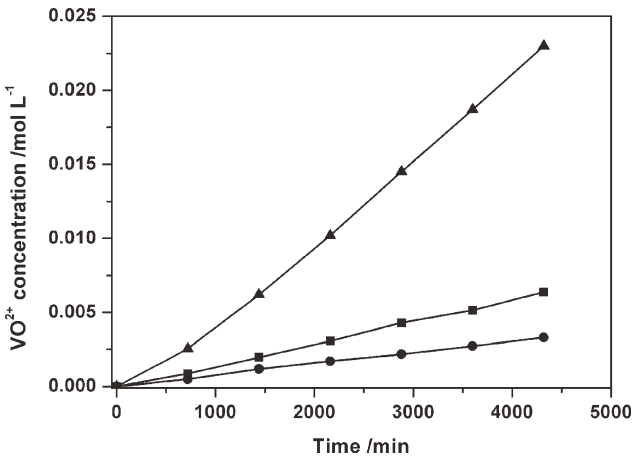

Figure 7. Dependency of VO^{2+} concentration in the right compartment as a function of time for SPI (-■-), SPI/CS (-●-) and Nafion® 117 (-▲-) membranes.

Table III. The Performance of SPI, SPI/CS, and Nafion® 117 Membranes in Single Cell

Membrane	Coulombic efficiency (%)	Voltage efficiency (%)	Energy efficiency (%)
SPI	94.0	92.2	86.7
SPI/CS	97.8	90.6	88.6
Nafion® 117	95.6	91.0	86.9

CONCLUSIONS

A novel sulfonated polyimide/chitosan (SPI/CS) composite membrane was prepared via an immersion and self-assembly method, and its application for VRB was investigated. FT-IR results verify the presence of both CS and SPI in the composite membrane. The cross-sectional SEM image of SPI/CS composite membrane clearly shows closely combined three-layer structure. Besides, the oxidative stability of SPI/CS composite membrane is visibly ameliorated through surface modification of SPI with CS. The proton conductivity of SPI/CS composite membrane also increases due to incorporation of sulfuric acid compared to the pristine SPI membrane. And the proton selectivity of SPI/CS composite membrane is higher than that of Nafion® 117 membrane. The VRB single cell using SPI/CS membrane reveals higher energy efficiency (88.6%) than that using Nafion® 117 membrane. All experimental results indicate that the SPI/CS composite membrane is a promising proton conductive membrane for VRB.

ACKNOWLEDGMENTS

This work was financially supported by Opening Foundation of Engineering Research Center of Biomass Materials, Ministry of Education (Southwest University of Science and Technology) (No. 10zxgk08) and Innovation Found of Southwest University of Science and Technology for Graduate Student (No. 11ycjj11). Special thanks will be given to Prof. S. H. Zhang from Dalian University of Technology for kindly providing the single cell tests.

REFERENCES

1. Sum, E.; Skyllas-Kazacos, M. J. *Power Sources* **1985,** *15*, 179.
2. Sum, E.; Rychcik, M.; Skyllas-Kazacos, M. J. *Power Sources* **1985,** *16*, 85.
3. Skyllas-Kazacos, M.; Rychcik, M.; Robins, R. G.; Fane, A. J.; Green, M. A. *J. Electrochem. Soc.* **1986,** *133*, 1057.
4. Rydh, C. J. *J. Power Sources* **1999,** *80*, 21.
5. Huang, K. L.; Li, X. Q.; Liu, S. Q.; Tan, N.; Chen, L. Q. *Renewable Energy* **2008,** *33*, 186.

6. Mohammadi, T.; Skyllas-Kazacos, M. J. *Appl. Electrochem.* **1997,** *27*, 153.
7. Mohammadi, T.; Skyllas-Kazacos, M. J. *Power Sources* **1995,** *56*, 91.
8. Li, X. F.; Zhang, H. M.; Mai, Z. S.; Zhang, H. Z. *Energy Environ. Sci.* **2011,** *4*, 1147.
9. Zhang, H. Z.; Zhang, H. M.; Li, X. F.; Mai, Z. S.; Zhang, J. L. *Energy Environ. Sci.* **2011,** *4*, 1676.
10. Tian, B.; Yan, C. W.; Wang, F. H. *J. Membr. Sci.* **2004,** *234*, 51.
11. Luo, X. L.; Lu, Z. Z.; Xi, J. Y.; Wu, Z. H.; Zhu, W. T.; Chen, L. Q.; Qiu, X. P. *J. Phys. Chem. B* **2005,** *109*, 20310.
12. Qiu, J. Y.; Li, M. Y.; Ni, J. F.; Zhai, M. L.; Peng, J.; Xu, L.; Zhou, H. H.; Li, J. Q.; Wei, G. S. *J. Membr. Sci.* **2007,** *290*, 174.
13. Luo, Q. T.; Zhang, H. M.; Chen, J.; You, D. J.; Sun, C. X.; Zhang, Y. J. *Membr. Sci.* **2008,** *325*, 553.
14. Mai, Z. H.; Zhang, H. M.; Li, X. F.; Bi, C.; Dai, H. J. *Power Sources* **2011,** *196*, 482.
15. Mai, Z. H.; Zhang, H. M.; Li, X. F.; Xiao, S. H.; Zhang, H. Z. *J. Power Sources* **2011,** *196*, 5737.
16. Chen, D. Y.; Wang, S. J.; Xiao, M.; Han. D. M.; Meng, Y. Z. *J. Power Sources* **2010,** *195*, 7701.
17. Chen, D. Y.; Wang, S. J.; Xiao, M.; Meng, Y. Z. *J. Power Sources* **2010,** *195*, 2089.
18. Jian, X. G.; Yan, C.; Zhang, H. M.; Zhang, S. H.; Liu, C.; Zhao, P. *Chin. Chem. Lett.* **2007,** *18*, 1269.
19. Zhang, S. H.; Yin, C. X.; Xing, D. B.; Yang, D. L.; Jian, X. G. *J. Membr. Sci.* **2010,** *363*, 243.
20. Yue, M. Z.; Zhang, Y. P.; Chen, Y. *Adv. Mater. Res.* **2011,** *239*, 2779.
21. Genies, C.; Mercier, R.; Sillion, B.; Cornet, N.; Gebel, G.; Pineri, M. *Polymer* **2001,** *42*, 357.
22. Osifo, P. O.; Masala, A. J. *Power Sources* **2010,** *195*, 4915.
23. Sonef, Y.; Ekdunge, D.; Simonsson, D. J. *Electrochem. Soc.* **1996,** *143*, 1254.
24. Xi, J. Y.; Wu, Z. H.; Teng, X. G.; Zhao, Y. T.; Chen, L. Q.; Qiu, X. P. *J. Mater. Chem.* **2008,** *18*, 1232.
25. Xing, D. B.; Zhang, S. H.; Yin, C. X.; Zhang, B. G.; Jian, X. G. *J. Membr. Sci.* **2010,** *354*, 68.
26. Smitha, B.; Anjali Devi, D.; Sridhar, S. *Int. J. Hydrogen Energy* **2008,** *33*, 4138.
27. Thanpitcha, T.; Sirivat, A.; Jamieson, A. M.; Rujiravanit, R. *Carbohydr. Polym.* **2006,** *64*, 560.
28. Seo, J. A.; Koh, J. H.; Roh, D. K.; Kin, J. H. *Solid State Ionics* **2009,** *180*, 998.